DOE/ER/53225--2

DE93 002522

PROGRESS REPORT

DOE Grant No. DOE-DE-FG03-86-ER-53225

Task IV

STUDIES OF PLASMA CONFINEMENT IN LINEAR AND RACETRACK MIRROR CONFIGURATIONS

Andras Kuthi

Alfred Y. Wong

University of California

Department of Physics

Los Angeles, CA 90024

May 28, 1989

DISCLAIMER

This report was prepared as an account of work sponsored by an agency of the United States Government. Neither the United States Government nor any agency thereof, nor any of their employees, makes any warranty, express or implied, or assumes any legal liability or responsibility for the accuracy, completeness, or usefulness of any information, apparatus, product, or process disclosed, or represents that its use would not infringe privately owned rights. Reference herein to any specific commercial product, process, or service by trade name, trademark, manufacturer, or otherwise does not necessarily constitute or imply its endorsement, recommendation, or favoring by the United States Government or any agency thereof. The views and opinions of authors expressed herein do not necessarily state or reflect those of the United States Government or any agency thereof.

MASTER

DISTRIBUTION OF THIS DOCUMENT IS UNLIMITED

TABLE OF CONTENTS

INTRODUCTION

During the period from November 1988 through April 1989 the experimental plasma physics program at UCLA produced several new results. The experiments were conducted on the toroidal RACETRACK device[1] (Fig.1). Generation of a steady-state high-beta field-reversed configuration[2] in one of the straight sections by the rotating electromagnetic wave technique[3] (Fig.2) is now routine and because of understanding gained in the course of experiments we succeeded in extending the range of operation.

The high beta field-reversed equilibrium generated by rotating magnetic fields can be described by the same two-fluid formalism as the earlier investigated high-beta mirror configuration, the electron and ion fluids both behaving as rigid rotors. We have verified explicitly the pressure balance relation by independent pressure and magnetic field measurements[4] even for this field reversed-configuration.

We have started experiments to extrapolate to higher field, better confined collisionless plasmas by studying field penetration and power deposition[5] by the rotating magnetic fields. Interestingly, the right-hand rotating component - the one rotating in the electron diamagnetic sense - fully penetrates the plasma while the left-hand rotating component is excluded but provides for most of the power input through the induced screening currents.

Studies of the equilibrium have been extended to spatial and temporal decay of the confining diamagnetic current. It has been observed, that the current decays on the resistive time scale due to electron-ion coulomb collisions. The plasma extends axially only to the end of the RF antenna, the spatial decay is related to the momentum input by the RF field and the momentum loss due to collisions and direct particle loss but since the angular

velocity itself does not decay on the same scale collective effects must be at play[6].

Toroidal current injection by a low-energy, high-current electron beam, similar to the DC helicity injection experiment by Ono et al[7], has been conducted in order to study the effects of mirror fields on toroidal currents and to reduce the neutral gas pressure for a given plasma density in the rotating field experiments. The design value of injected beam current has been achieved, and studies of mirror field and scattering effects has been initiated[8].

REVERSED FIELD CONFIGURATION

We can routinely generate reversed-field configurations in a straight-section of RACETRACK (Fig.3). This configuration is stable, steady-state, and conforms to the theoretical model based on rigid electron and ion fluid rotation. By using a strong electron beam preionization technique the configuration can now be generated at reduced neutral gas pressures (5×10^{-5} torr A or 10^{-4} torr H_2), and consequently at higher axial magnetic fields (up to 25 G). The better RF power utilization at low pressures allows the higher total current generation (up to 2.5 kA). Representative profiles of magnetic field, diamagnetic (poloidal) current density, and electron density as a function of radius are presented in Fig.4. About 40 % field reversal on axis is achieved. The electron temperature profile is flat, independent of the radius in zero order (Fig. 5), but there is a slight tendency to adiabaticity, that is, the temperature has a weak peak at the density minimum and a slight minimum at the density peak. Using the isothermal approximation is, however, adequate for the equilibrium fit.

FIELD PENETRATION

In Rotating magnetic field driven configurations a key question is the efficiency of the current drive, the amount of power needed to drive a given total current. In order to gain better understanding of the current drive process and the scaling relations which allow predictions of operating parameters for high temperature collisionless plasmas, details of power deposition and field penetration were measured on Racetrack.

When the RF power and thus the rotating field amplitude is above the electron magnetization threshold (2 G), complete field penetration of the right-hand component takes place. This can be seen from Fig.6, the radial distribution of relative phase and magnitude between the radial and azimuthal components of the measured magnetic field. The field inside the plasma is always right-hand circularly polarized, independent of the antenna polarization. The magnitude of the right rotating field on axis corresponding to the radius of the Lissajous figure is 4 G.

POWER DEPOSITION

The power deposition profile derived from the probe signals, figure 7, is consistent with the total power leaving the antenna, and with the fact that the left-hand rotating field is excluded thus depositing power mainly in the outer plasma regions by the screening currents. The outer plasma layers are somewhat slower rotating than the field and the resultant increase of momentum input by the right handed wave compensates the token amount of torque directed oppositely by the left wave. The total power input is about ten times larger than the power dissipated by the diamagnetic current alone. As a consequence of preferential power input by the left-rotating wave and momentum input by

the right-handed wave the antenna loading is very sensitive to the antenna polarization.

SPATIAL AND TEMPORAL DECAY

Studies of the equilibrium have been extended to spatial and temporal decay of the confining diamagnetic current. It has been observed, that the current decays on the resistive time scale due to electron-ion coulomb collisions. The high-beta plasma extends axially only to the end of the RF antenna (fig.4), the spatial decay is related to the momentum input by the RF field and the momentum loss due to collisions and direct particle loss but since the angular velocity itself does not decay on the same scale as the angular momentum (fig.8) collective effects must be at play. A possible candidate for axial angular velocity transfer is the generation of a radial electric field. This effect is being investigated further, since it may provide a beneficial contribution to toroidal confinement of the particles outside the separatrix.

ELECTRON BEAM INJECTION

The field reversal experiments are at the RF power limit given by the present RF power amplifiers. However, calculations show, that only about 20 % of the RF power absorbed by the plasma is needed for the azimuthal electron momentum input, the rest is used for ionization and transport losses. Therefore, an experimental program has been conducted to relieve the RF power supplies from ionization duties by a separate plasma production scheme. A low energy high-current electron beam injection in the toroidal direction, similar to the DC helicity injection scheme used by Ono et al, has been developed. This electron

beam has the additional advantage of providing a respectable free electron source as well, independent of plasma loss processes, and thus it enabled us to operate at reduced neutral gas densities leading to higher equilibrium electron temperatures which have reduced further the requirement for RF power. If this scheme reaches its full potential, confinement in the toroidal sections will become possible by the rotational transform generated by the toroidal beam current.

The LaB_6 beam source has reached the design level of 50 A beam current at 500 V beam energy. In the near future the beam energy will be extended to 1 kV. Measurements of circulating toroidal current indicate that, due to the cylindrical cathode geometry, only a small fraction of electrons are born in the local mirror loss-cone and thus contribute to the toroidal current. This deficiency is presently being cured by installation of a flat cathode. The present cathode will be moved to a toroidal section temporarily to check if other effects are present limiting the total toroidal current in a single pass.

REFERENCES

[1] "Racetrack: A Novel Device for Basic Research on Magnetized Plasmas" A. Kuthi, H. Zwi, L. Schmitz, D. Chelf and A.Y. Wong, Rev. Sci. Instrum. 57 (1986) 2720.

[2] "Steady-state field reversed configuration equilibrium in RACETRACK" H. Zwi, A. Kuthi, A.Y. Wong, B. Wells and S. Loucks, UCLA PPG 1239 (1989).

[3] "Stability of a Rotating Field Generated Mirror Equilibrium" A. Kuthi, Physics Letters A, 127 (1988) 431.

[4] "Observation of Stable High-Beta Axisymmetric Plasma Equilibrium" A. Kuthi, H. Zwi, L. Schmitz, and A.Y. Wong, submitted to Phys. Fluids (1988).

[5] "Power deposition and field penetration in a field-reversed configuration generated by rotating magnetic fields" A. Kuthi, H. Zwi, B. Wells and A.Y. Wong, 8th Topical conf. on Radiofrequency heating in plasmas, Irvine CA (1989) and UCLA PPG 1240 (1989).

[6] "Spatial and temporal decay of a field-reversed configuration generated by rotating electromagnetic fields" A. Kuthi, H. Zwi, B. Wells, and A.Y. Wong, Bull. Am. Phys. Soc. 33 (1988) 2002, paper 5W6.

[7] "Formation and Maintenance of a Tokamak Discharge via DC Helicity Injection" M. Ono et al. PPPL report.

[8] "Electron beam current injection in RACETRACK" B. Wells, A. Kuthi, H. Zwi and A.Y. Wong, Bull. Am. Phys. Soc. 33 (1988) 1947, paper 4P4.

FIGURE CAPTIONS

Fig. 1. The RACETRACK experiment and diagnostic layout.

Fig. 2. The rotating field antennas and the currents generated by the fields.

Fig. 3. Schematic configuration of the present reversed field experiment.

Fig. 4. Radial profiles of axial magnetic field, diamagnetic current density, and electron density in the reversed-field configuration.

Fig. 5. Radial profile of the electron temperature as measured by floating double probes. Note the tendency to inverse variation with respect to the density.

Fig. 6. Phase and Amplitude profile of the rotating field. Notice that on axis the field is circularly polarized.

Fig. 7. Distribution of RF power deposition by the screening plasma currents.

Fig. 8. Spatial decay of the plasma equilibrium. Notice the radius being invariant, indicating constant angular velocity, but the peak density decays sharply showing loss of fluid angular momentum.

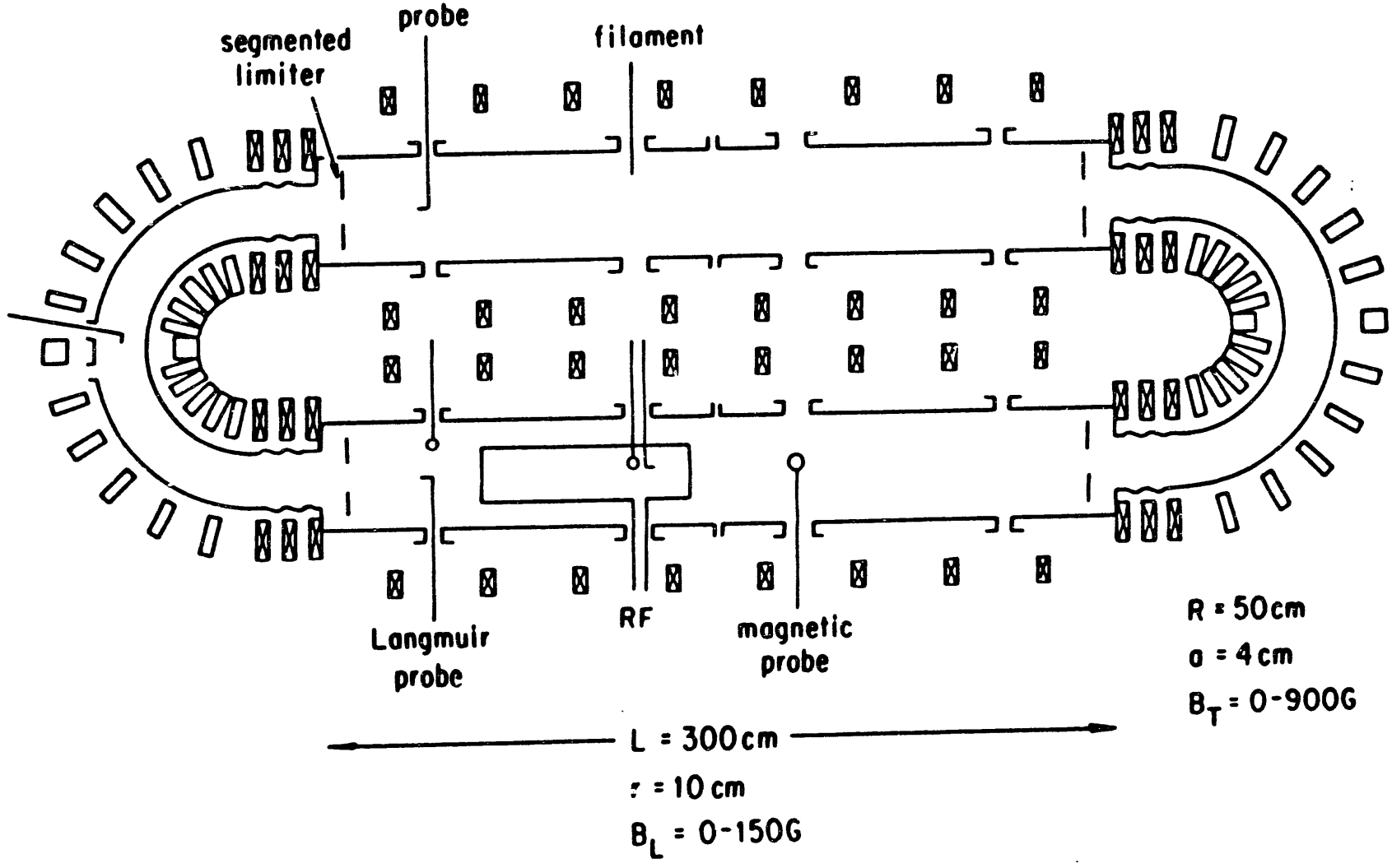
segmented limiter
probe
filament
Langmuir probe
RF
magnetic probe
R = 50cm
a = 4cm
B_T = 0-900G
L = 300cm
r = 10cm
B_L = 0-150G

Figure 1

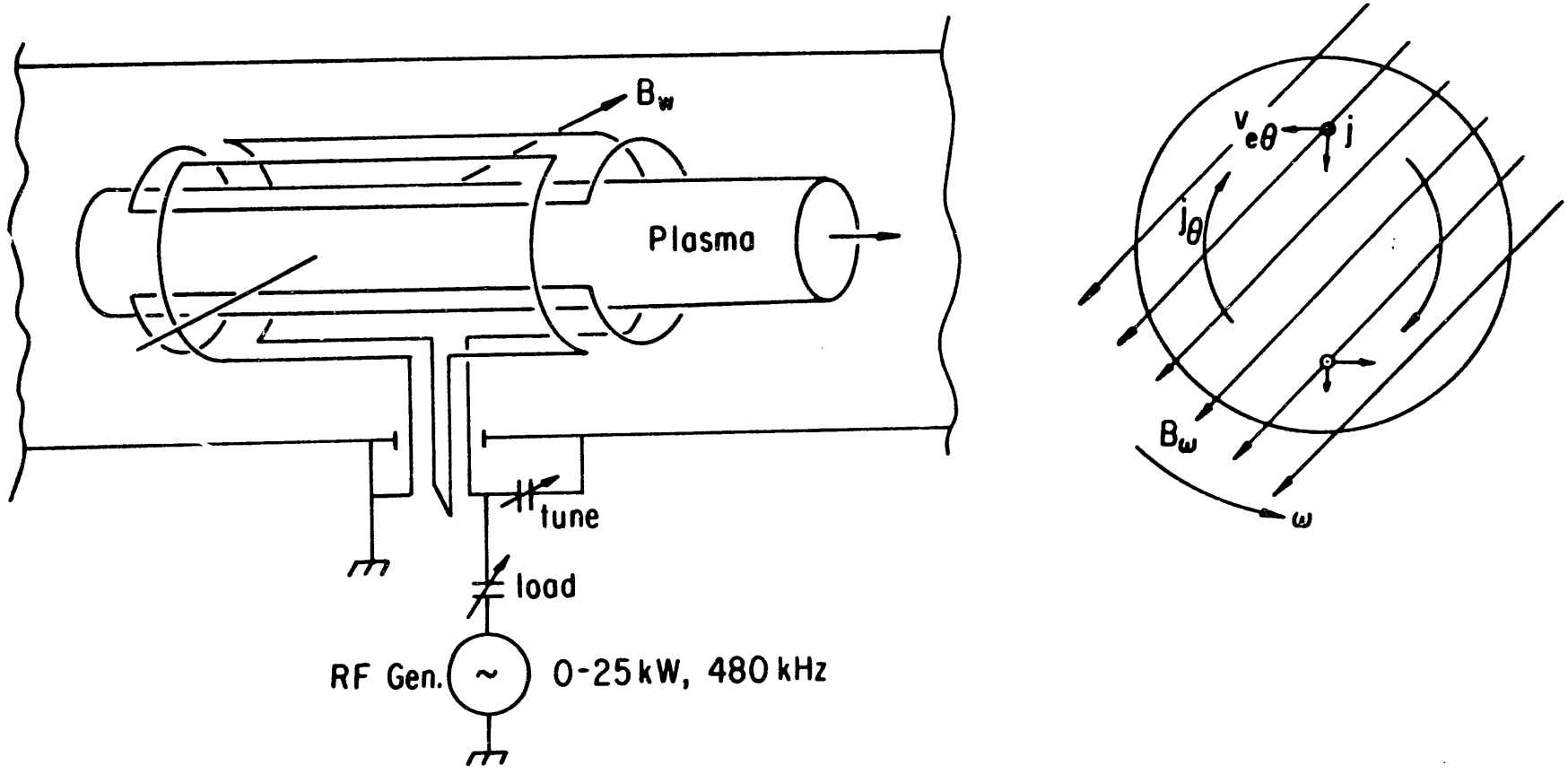
B_w
Plasma
tune
load
RF Gen.
~
0-25 kW, 480 kHz
$v_{e\theta}$
j
j_θ
B_ω
ω

Figure 2

Present Reversed Field RACETRACK Configuration

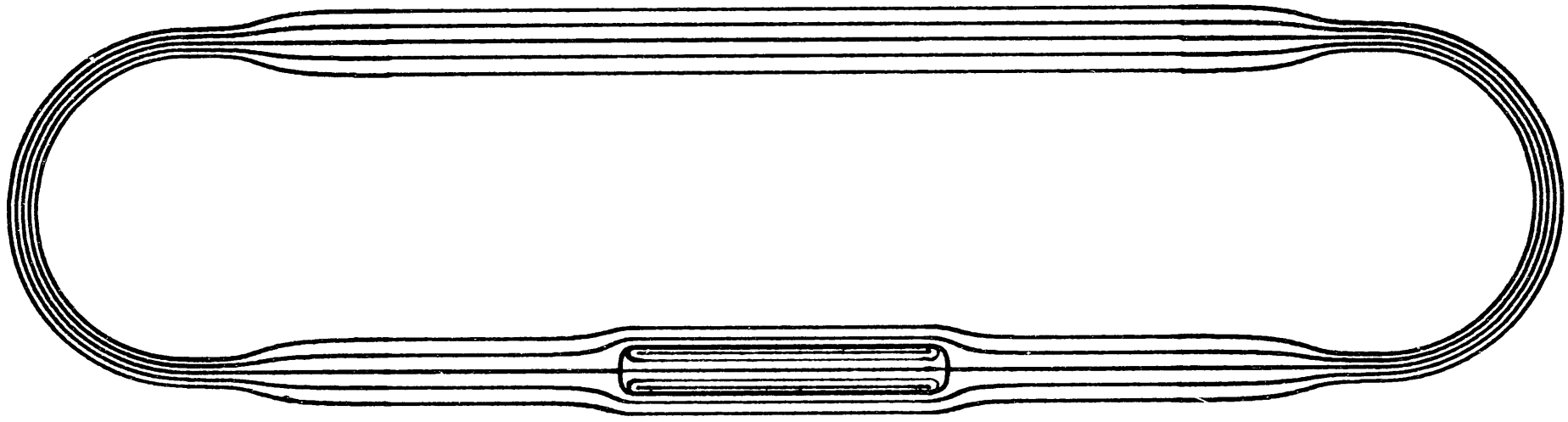

1 meter

Figure 3

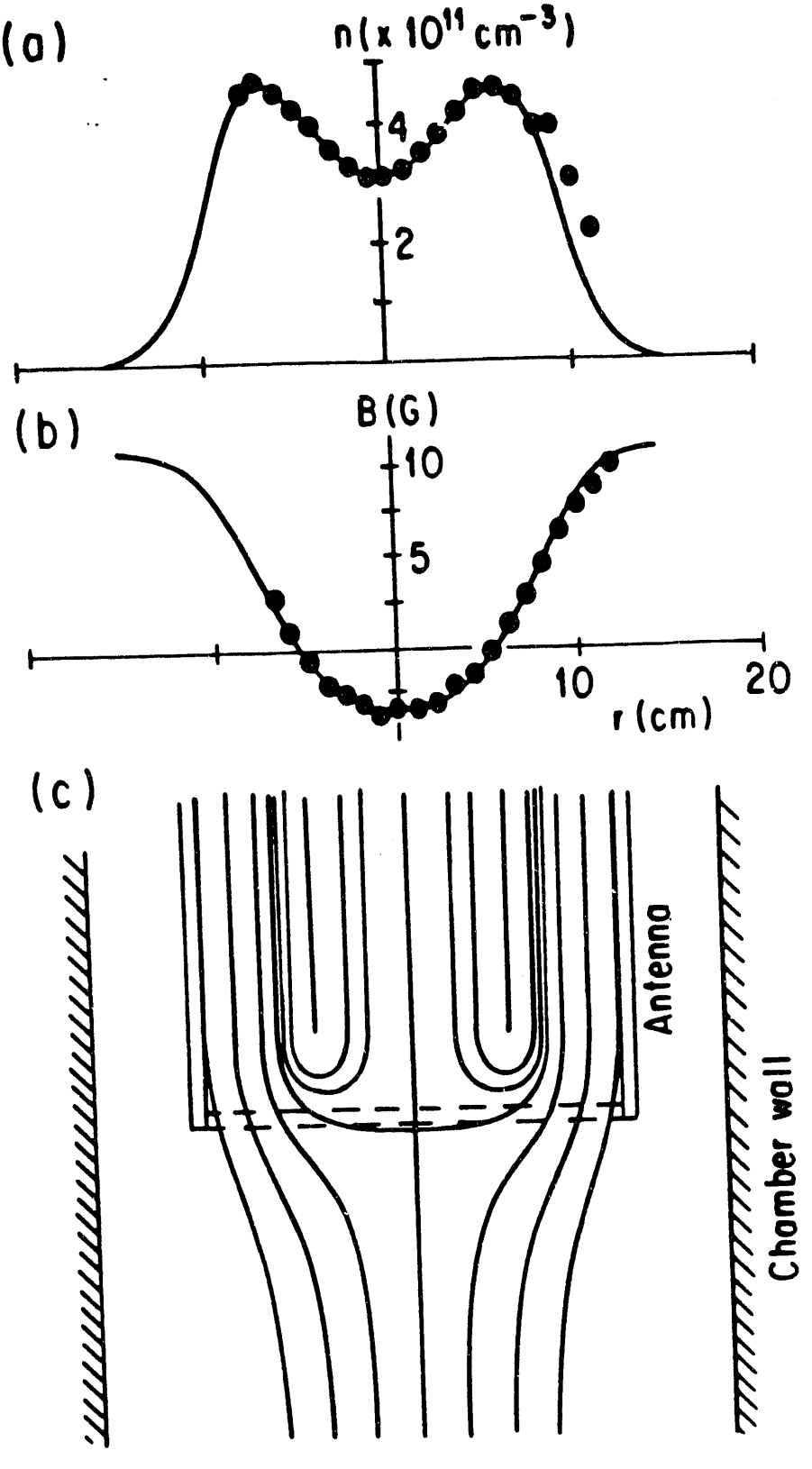

Figure 4

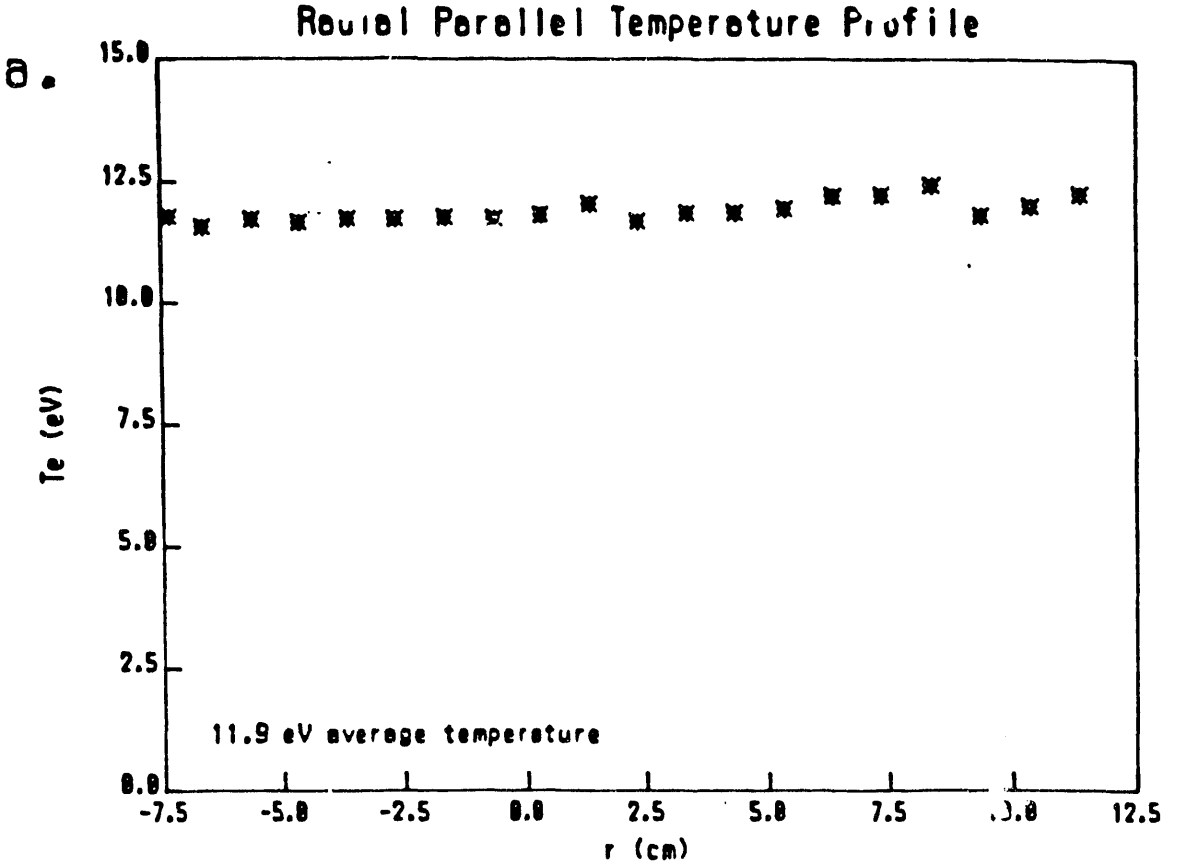
a.
Radial Parallel Temperature Profile
15.0
12.5
10.0
7.5
5.0
2.5
0.0
Te (eV)
11.9 eV average temperature
-7.5
-5.0
-2.5
0.0
2.5
5.0
7.5
10.0
12.5
r (cm)

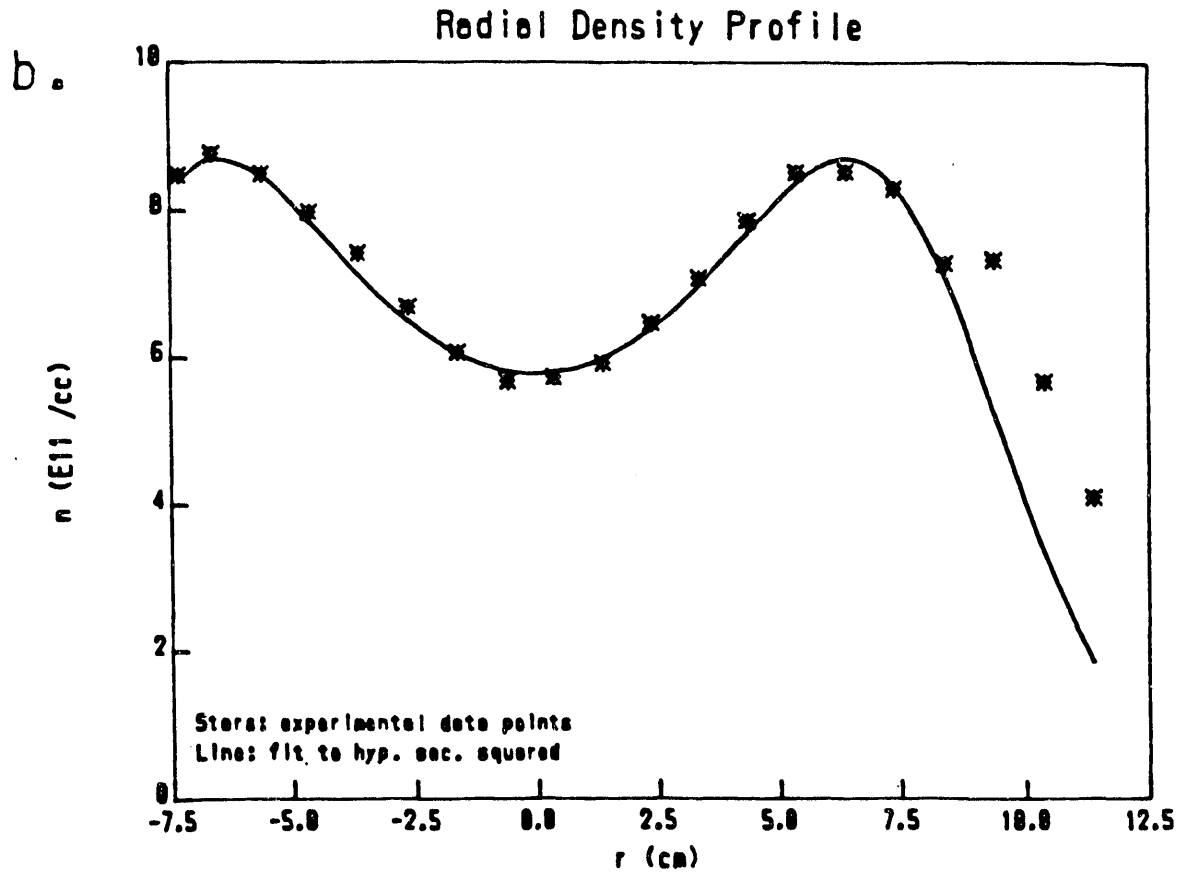
b.
Radial Density Profile
10
8
6
4
2
0
n (E11 /cc)
Stars: experimental data points
Line: fit to hyp. sec. squared
-7.5
-5.0
-2.5
0.0
2.5
5.0
7.5
10.0
12.5
r (cm)

Figure 5

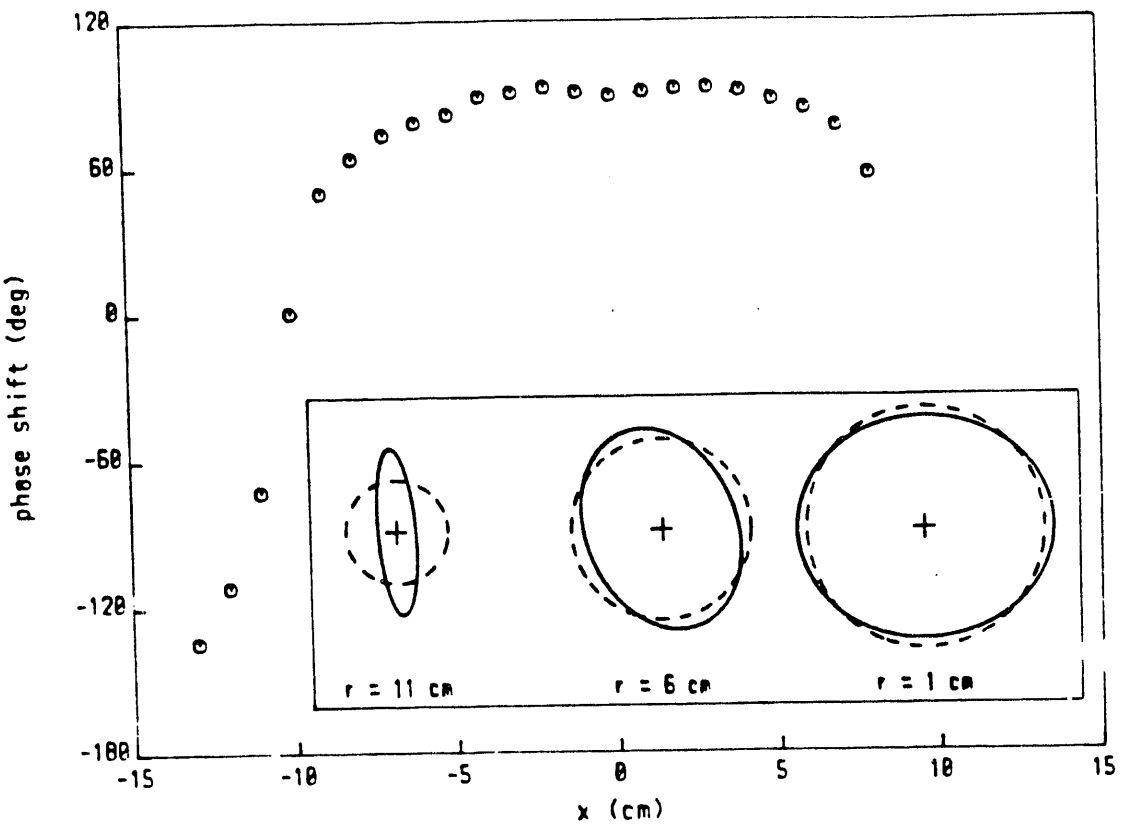

Phase and amplitude profile of the rotating field.

Figure 6

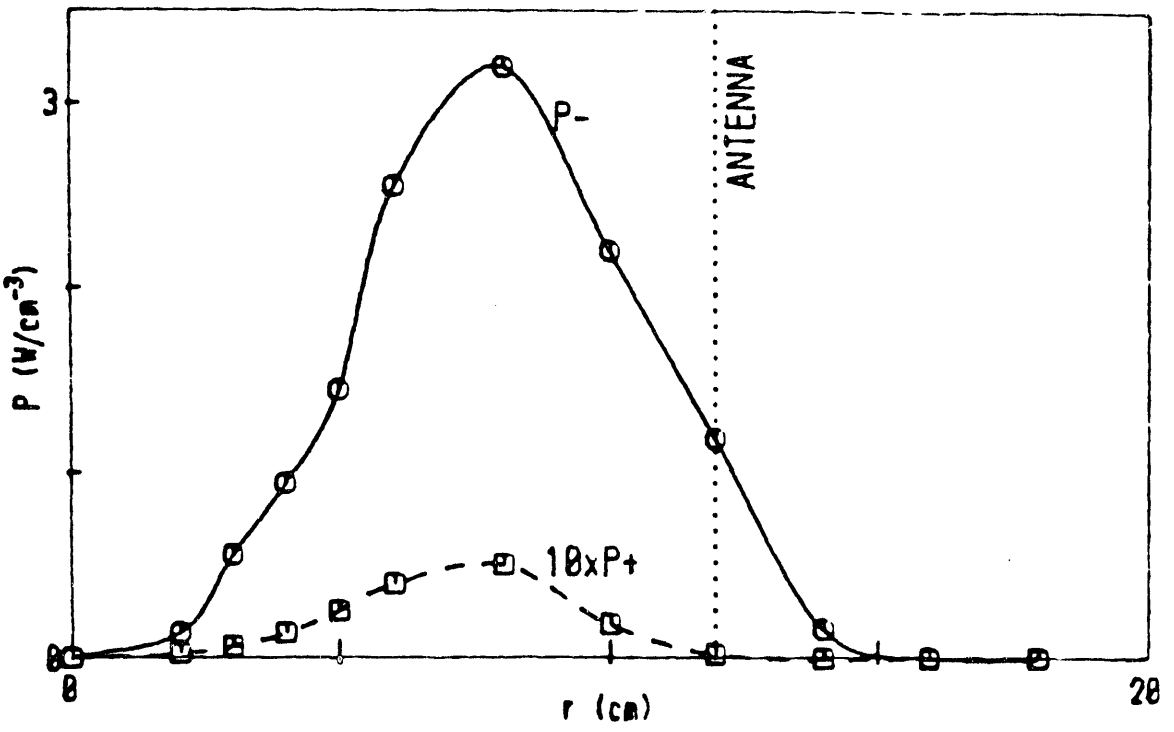

Distribution of RF power deposition by the screening plasma currents.

Figure 7

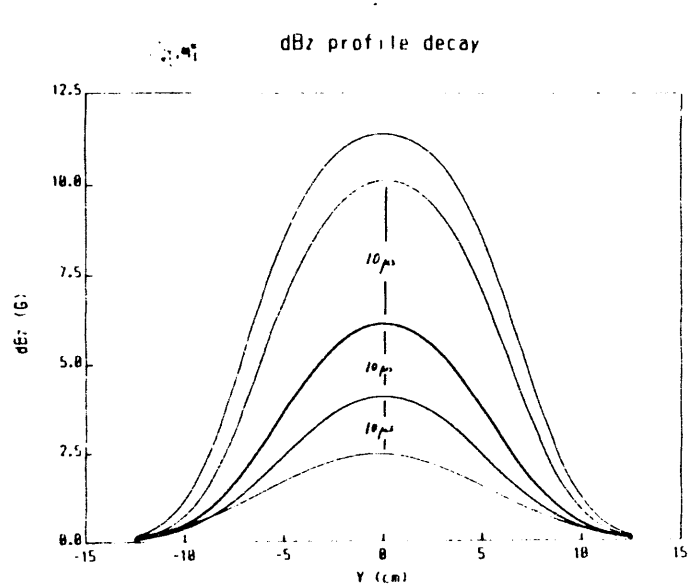
dBz profile decay
dBz (G)
Y (cm)

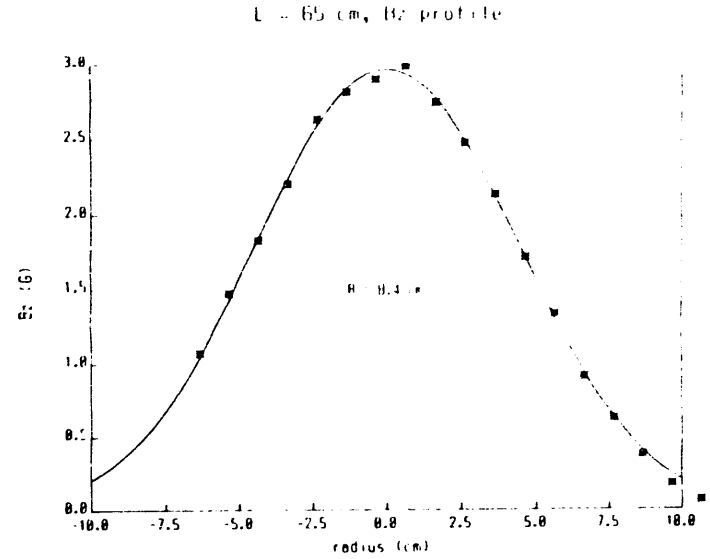
L = 65 cm, Bz profile
Bz (G)
radius (cm)

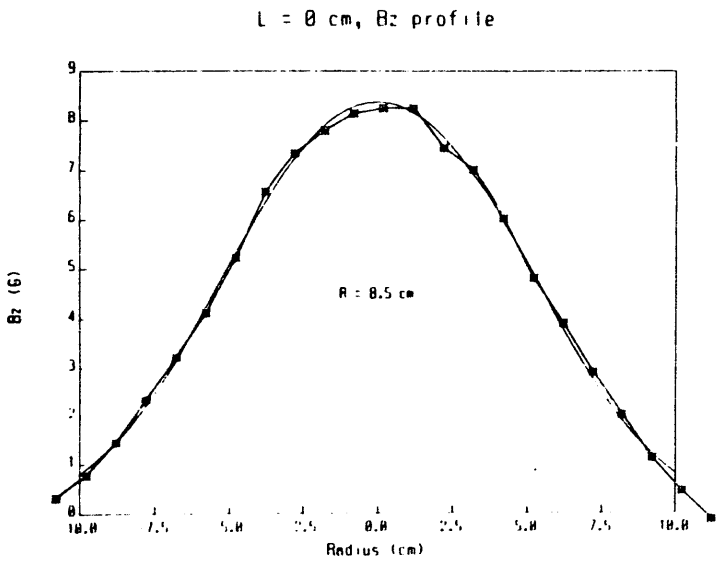
L = 0 cm, Bz profile
Bz (G)
R = 8.5 cm
Radius (cm)

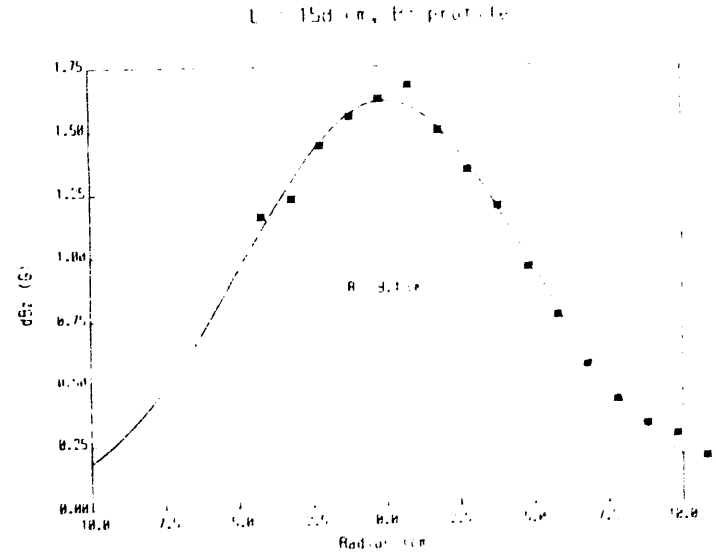
dBz (G)

Figure 8

END

DATE
FILMED
12/15/92